BIOLOGY, MEDICINE, & NATURAL PRODUCT CHEMISTRY ISSN 2089-6514 (paper)
Volume 15, Number 1, April 2026 | Pages: 1713-1723 | DOI: 10.14421/biomedich.2026.151.1713-1723 ISSN 2540-9328 (online)

Green Synthesis of Iron Nanoparticles using *Ficus capensis* Stem Bark Extract: Characterization, Antioxidant and Antibacterial Evaluations

Uchenna Benjamin Okeke[1]*, Ejiro Dowe[2], Oscar Ifeanyichukwu Onyemaobi[1], Bako Wunia'h[3], Wande Michael Oluyemi[1]

[1]Department of Pharmaceutical and Medicinal Chemistry, College of Pharmacy, Afe Babalola University, Ado-Ekiti, Nigeria.
[2]Department of Pharmaceutical Microbiology and Biotechnology, Faculty of Pharmacy, Delta State University, Abraka, Nigeria.
[3]Department of Pharmaceutics and Pharmaceutical Technology, College of Pharmacy, Afe Babalola University, Ado-Ekiti, Nigeria.

Corresponding author*
okeke.uchenna@abuad.edu.ng

Manuscript received: 30 April 2026. Revision accepted: 19 June 2026, Published: 02 September 2026.

Abstract

Biogenically derived metal nanoparticles have garnered considerable interest as eco-friendly nanomaterials possessing distinctive properties that support the development of sustainable therapeutic alternatives. This study evaluated the antioxidant and antibacterial activities of iron nanoparticles (FeNPs) synthesized via a green route using *Ficus capensis* stem bark extract. The plant part was collected from its natural habitat, authenticated, and extracted with 80% methanol. Phytochemical analysis was performed on the extract following standard protocols. FeNPs were prepared using a mixture of 0.1 M ferric chloride and the extract. The synthesized nanoparticles were characterized by UV–visible spectroscopy, Fourier transform infrared spectroscopy, scanning electron microscopy, and X-ray diffraction. Their antioxidant capacity was assessed using the DPPH (2,2-diphenyl-1-picrylhydrazyl) radical scavenging assay (RSA), while antibacterial activity and minimum inhibitory concentrations (MICs) were determined according to established microbiological methods. The synthesized FeNPs were found to be agglomerated and non-spherical in nature, exhibiting substantial DPPH RSA with an IC_{50} of 6.474 ± 0.59 µg/mL. The FeNPs showed antibacterial action against *Escherichia coli*, *Klebsiella pneumoniae*, and *Staphylococcus aureus*, with limited activity against *Bacillus subtilis* and *Pseudomonas aeruginosa*. These results underscore the potential of *F. capensis*-derived FeNPs as environmentally benign therapeutic agents for addressing oxidative stress and certain bacterial infections.

Keywords: Antibacterial activity; Antioxidants; Green synthesis; Nanoparticles; Nanostructure.

INTRODUCTION

Nanoparticles, which are particles with dimensions approximately 1–100 nm, frequently exhibit size-dependent physicochemical properties distinct from bulk materials. Their morphologies vary widely—spherical, cylindrical, tubular, conical, hollow-core, spiral, planar, or irregular—and surface topography may be either uniform or heterogeneous. Structurally, nanoparticles can consist of single or multiple crystalline domains that are either dispersed or aggregated, and they may present as crystalline or amorphous phases (Machado et al., 2015). To enhance functional performance while reducing production costs, numerous synthesis methods have been developed and refined; process parameters are routinely adjusted to yield nanoparticles with tailored mechanical, chemical, optical, and physical properties (Cho et al., 2013). Both chemical and biological routes are employed for nanoparticle fabrication. Conventional chemical syntheses frequently involve hazardous reagents that can adsorb onto particle surfaces and pose environmental and health concerns. In contrast, biogenic approaches—using microorganisms, enzymes, fungi, or plant extracts—offer a more sustainable alternative to chemical and physical methods (Ghosh et al., 2021; Tehri et al., 2022; Karunakaran et al., 2023). The development of such eco-friendly synthesis strategies has therefore become a prominent focus within nanotechnology, given their broad applicability (Karunakaran et al., 2023; Osman et al., 2024).

Iron oxide nanoparticles (FeNPs) have gained significant attention as versatile nanomaterials due to their broad spectrum of applications. These nanostructures exist in several crystalline forms, including maghemite (γ-Fe_2O_3), magnetite (Fe_3O_4), and hematite (α-Fe_2O_3), each of which exhibits distinctive magnetic and catalytic properties. Such characteristics have positioned FeNPs as valuable tools in biomedical, bioengineering, and clinical contexts (Sahoo et al., 2010). Their potential in drug delivery, diagnostic imaging, and antimicrobial development is particularly noteworthy, as their intrinsic antioxidant and antimicrobial activities may contribute to novel therapeutic strategies for oxidative stress-related disorders while also advancing healthcare and food safety initiatives (Salehirozveh et al., 2024).

Beyond iron oxide, a wide range of metal nanoparticles (MNPs)—including silver, gold, zinc oxide, selenium, copper, cobalt/cobalt oxide, and aluminium oxide—have been extensively investigated for their efficacy against multidrug-resistant bacterial pathogens (Mishra et al., 2022). The physicochemical attributes of these nanoparticles, such as their nanoscale dimensions, morphology, surface charge, and functionalization, enable them to act as alternative antimicrobial agents. Their mechanisms of action typically involve disruption of bacterial membrane integrity and potential inhibition of biofilm formation, induction of reactive oxygen species (ROS), modulation of host immune responses, and interference with intracellular processes such as RNA and protein synthesis. Collectively, these properties highlight the promise of MNPs as innovative strategies to mitigate the growing challenge of antimicrobial resistance (Mishra et al., 2022; Wahab et al., 2023).

Numerous plant species have been reported as effective biological agents for the synthesis of iron nanoparticles. Among them, *Ficus capensis* has emerged as a particularly promising candidate due to its rich phytochemical profile, which includes compounds with strong reducing properties that can convert ferrous sulphate into metallic nanoparticles (Esievo et al., 2018; Mgbemena et al., 2022). Commonly referred to as the "bush fig tree," *F. capensis* belongs to the Moraceae family and is widely recognized in Nigeria under various local names, including Akokoro (Igbo), Opoto (Yoruba), and Uwaraya (Hausa) (Achi et al., 2017; Omodamiro et al., 2021). This deciduous tree is characterized by its broad green leaves and expansive root and branch system. Pharmacological investigations have documented its diverse bioactivities, encompassing antibacterial, antioxidant, immune-enhancing, gastrointestinal-relaxant, and tocolytic properties (Esievo et al., 2018). Despite its promising attributes, the plant's potential as a bio-reductant for iron nanoparticle synthesis is underexplored. Employing the stem bark extract for the green synthesis of FeNPs constitutes an innovative approach that could both enhance the plant's medicinal significance and advance sustainable nanotechnology. Also, evaluating the antioxidant and antibacterial activities of the synthesized FeNPs may support the development of biocompatible therapeutic agents with potential efficacy against oxidative stress and drug-resistant microbial infections.

MATERIALS AND METHODS

Equipment and Reagents

Centrifuge 8000 rpm (Biobase, China), UV-visible spectrophotometer (Biobase BK-D560, China), Fourier Transform Infrared (FTIR) spectrophotometer (Agilent Cary 630, USA), Scanning electron microscope (Phenom ProX, The Netherlands), XRD machine (Rigaku MiniFlex 600, Japan), Iron(III)chloride hexahydrate (97.0%) (LobaChemie, India), Sodium hydroxide (Molychem, India).

Collection and extraction of plant material

Ficus capensis stem bark was collected from its natural habitat in Ado-Ekiti, Nigeria, in October 2024 (Figure 1) by Mr. Felix Omotayo, a Taxonomist in the Department of Plant Science and Biotechnology, Ekiti State University, Ado-Ekiti, where a herbarium specimen of the plant material (voucher number: UHAE2023081) was deposited. The freshly collected plant part was rinsed with distilled water, dried in the shade, and pulverized into fine particles using a milling machine. The powdered material (25 g) mixed with 250 mL of distilled water in a 500 mL beaker was heated at 60°C for 30 min and cooled thereafter to room temperature. The solution was filtered with Whatman no. 1 filter paper to obtain a clear orange-coloured extract, which was used immediately for nanoparticle synthesis.

Preliminary phytochemical analysis of the extract

Phytochemical screening of *F. capensis* stem bark extract was carried out using standard methods described by Sofowora (1993) and Trease and Evans (2003). The samples were screened for alkaloids, flavonoids, phenolics and tannins, terpenoids, glycosides, saponins, anthraquinones, carbohydrates, and proteins.

Green synthesis of iron nanoparticles

To synthesize the iron nanoparticles (FeNPs), a freshly prepared 0.01 M solution of $FeCl_3.6H_2O$ was added dropwise to 50 mL of *F. capensis* extract solution with continuous stirring. The pH of the mixture was adjusted to basic (pH of 11) using a few drops of 0.1 M NaOH. The mixture was stirred for 1 h and observed for a color change from an orangish-brown solution to an intense black precipitate, indicating the formation of nanoparticles. The product was centrifuged at 8000 rpm for 15 min, the solid sediment collected and washed with ethanol and distilled water (1:1) three times to remove any unreacted salt and metabolites. The resultant pellet was collected and oven-dried at 90ºC for 2 h to obtain black-colored, purified iron nanoparticles (Bhuiyan et al., 2020). Figure 2 shows the steps (left to right) for the iron nanoparticles synthesis.

Figure 1. *F. capensis* in its natural habitat (NMPP, 2026)

(a) (b) (c)

Figure 2. (a) *F. capensis* stem bark extract combined with (b) $FeCl_3.6H_2O$ solution to produce (c) FeNPs.

Characterization of FeNPs

A comprehensive characterization of the FeNPs was conducted using multiple analytical techniques, including ultraviolet-visible spectroscopy (UV-vis), Fourier-transform infrared spectroscopy (FTIR), scanning electron microscopy (SEM), and X-ray diffraction (XRD).

Ultraviolet-visible spectroscopy

UV-vis spectroscopy, an important technique used to confirm the synthesis of nanoparticles, was employed to determine the optical properties of the nanoparticle molecules. The UV-vis absorption spectrum of the FeNPs solution was scanned within the wavelength range of 200 to 700 nm, using a Biobase BK-D560 UV-visible spectrophotometer.

Fourier transform infrared spectroscopy

A deeper understanding of the chemical composition and bonding interactions in the compound was assessed by Attenuated Total Reflectance Fourier Transform Infrared Spectroscopy (ATR-FTIR), using an Agilent Cary 630 FTIR spectrophotometer (USA). The nanoparticles were placed directly onto the ATR crystals, and pressure was applied to ensure good contact with the crystal. The spectrum was collected by shining an infrared beam onto the crystal and measuring the reflected light as a function of wavelength by scanning over a wavenumber range of 400 to 4000 cm^{-1}. The FTIR spectrum obtained was analyzed to determine the functional groups present in the nanoparticles' molecules.

X-ray diffraction

To determine the crystalline nature and average size of the nanoparticles, X-ray diffraction (XRD) analysis was performed using Rigaku MiniFlex 600. Were measurements carried out on a reflection–transmission spinner stage in Theta-Theta configuration, scanning the 2θ range from 20° to 80°, providing essential structural information.

Scanning electron microscopy

Scanning electron microscopy (Phenom ProX, PhenomWorld, Eindhoven, The Netherlands) was employed to investigate the nanoparticles and determine their surface morphology. Samples were mounted on a double-sided adhesive tape affixed to a specimen stub, sputter-coated with a 5 nm gold layer using a Quorum

Technologies Q150R coater, and introduced into the SEM chamber. Initial focusing and minor adjustments were performed with the NaVCaM system before switching to SEM mode; the instrument then auto-optimized focus and brightness/contrast, and micrographs at various magnifications were obtained (Okafor et al., 2024).

***In-vitro* antioxidant activity of FeNPs**

The antioxidant activity of the FeNP was assessed by the method described by Sánchez-Moreno et al. (1998). A 1 mL portion of DPPH solution (0.05 mg/mL) prepared in methanol was added to the weighed amount of FeNPs and ascorbic acid at graded concentrations of 3.13, 6.25, 12.50, 25.00, 50.00, and 100.00 µg/mL, in triplicate. The samples were kept in the dark for 30 minutes, and thereafter, their absorbance was measured spectrophotometrically at 517 nm. The radical scavenging activities of the samples expressed as percentage inhibition of DPPH radical were calculated as follows:

$$\text{DPPH radical scavenging activity (\%)} = \frac{(\text{A control} - \text{A test})}{\text{A control}} x\ 100$$

Where '$A_{control}$' is the absorbance shown by the control (0.05mg/ml DPPH solution) and 'A_{test}' is the absorbance by the test sample (extract + 0.05mg/ml DPPH solution). The IC_{50} of the FeNPs was calculated from the 'equation of a straight line' of the absorbance-concentration curve.

Determination of antibacterial activity

Preparation of the microorganisms

Clinical isolates of bacterial strains sourced from the Microbiological Bank of the Department of Pharmaceutical Microbiology and Biotechnology, College of Pharmacy, ABUAD, were used in the study, which include Gram-positive (*Bacillus subtilis, Escherichia coli, Staphylococcus* aureus) and Gram-negative (*Pseudomonas aeruginosa, Klebsiella pneumonia*) bacterial strains.

Antibacterial screening

The modified Kirby–Bauer agar-well diffusion method was employed (Hossain, 2024). Wells (10 mm diameter) were aseptically bored into Mueller–Hinton agar plates using a flamed cork borer; the well bases were sealed with molten Mueller–Hinton agar and each well was loaded with 0.1 mL of FeNP suspension at 125 µg·mL^{-1} and 250 µg·mL^{-1}. Amoxicillin–clavulanic acid (30 µg·mL^{-1}) and distilled water served as the positive and negative controls, respectively. Test organisms were sub-cultured into nutrient broth and adjusted to the 0.5 McFarland turbidity standard by 1:100 dilution prior to seeding. Sterile swabs were dipped into the standardized suspensions and used to evenly inoculate the agar surface. Plates were incubated at 37 °C for 24 h, after which inhibition-zone diameters were measured and interpreted against established criteria to determine microbial susceptibility to the FeNPs.

Minimum inhibitory concentration

The minimum inhibitory concentration (MIC) of the FeNPs was determined using the agar dilution method. Agar was prepared according to standard protocols, and 1.0 g of the synthesized nanoparticles was suspended in an appropriate volume of distilled water to form a stock suspension. Aliquots of this suspension were incorporated into molten agar at varying volumes to produce a series of FeNP concentrations by serial dilution. The nanoparticle-containing agar was poured into sterile Petri dishes and allowed to solidify. Test organisms, standardized to the 0.5 McFarland turbidity standard, were then spotted onto the solidified media. Each experimental set included positive and negative controls. Plates were incubated at 37 °C for 24 h in triplicate, after which growth was assessed. The MIC was recorded as the lowest FeNP concentration that completely inhibited visible growth of the test organism (Wiegand et al., 2008).

RESULTS AND DISCUSSION

Result

Phytochemical constituents of *F. capensis* stem bark extract

Table 1 shows the various classes of phytochemicals found in *F. capensis* stem bark extract, which include saponins, tannins, phenolics, flavonoids, and terpenoids. These phytochemicals are essential for the biological activities observed in the plant and play an important role as reducing agents and stabilizers in the stages of nanoparticle synthesis.

Table 1. Phytochemical constituents of *F. capensis* stem bark extract.

Phytochemical	Result
Alkaloids	-
Phenols and tannins	+
Flavonoids	+
Saponin	+
Glycosides	+
Steroids	+
Protein and amino acid	-
Reducing sugars	+
Carbohydrates	+

"+" – Present; "-" - Absent

Characterization of the green-synthesized FeNP

UV–visible spectrophotometric analysis

The UV–vis spectrum of the synthesized FeNPs presented in Figure 3 showed a λmax of 320.7 nm, indicating electronic transitions of the molecules of the nanoparticles due to absorption of the ultraviolet region of light.

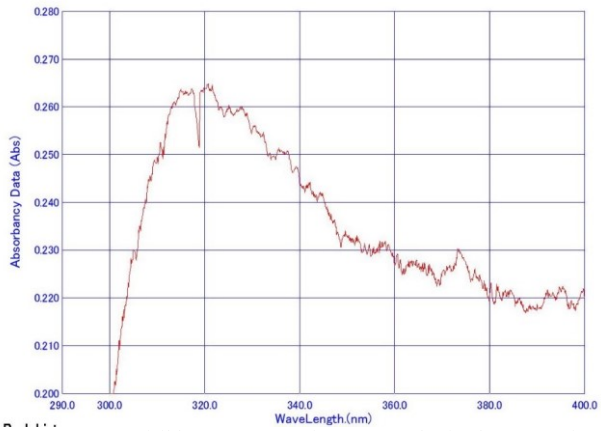

Figure 3. UV-visible spectrum of green-synthesized FeNPs from *F. capensis*

Fourier transform infrared spectroscopy

Various phytochemicals play a role in the capping and stabilization of nanoparticles produced through biosynthesis. FTIR serves as an effective method for examining the functional groups that contribute to the capping of nanoparticles. The FTIR spectrum of the FeNPs, presented in Figure 4, shows notable absorption bands at 3254 cm^{-1}, 2922 cm^{-1}, 1603 cm^{-1}, and 1018 cm^{-1}, confirming the capping of FeNPs by the phytochemicals present in the plant extract.

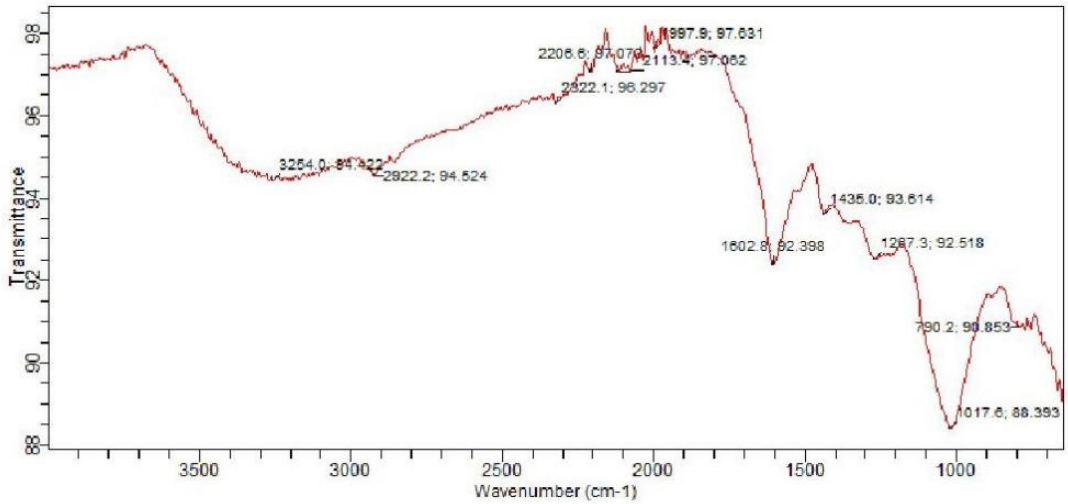

Figure 4. FTIR spectrum of the green-synthesized FeNPs showing the various absorption bands.

Scanning electron microscopy

SEM functions as a high-resolution imaging method, utilizing an electron beam to scan a sample's surface and generate detailed images that reveal the sample's structural morphology and size. The SEM image depicted in Figure 5 revealed the presence of non-spherical amorphous nanostructures.

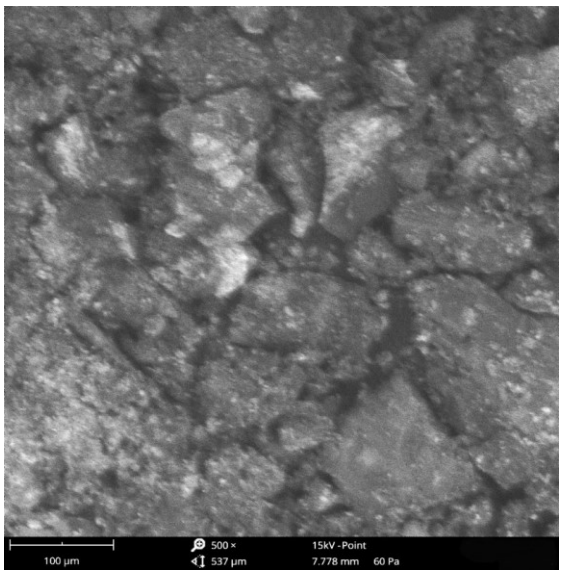

Figure 5. SEM of green-synthesized FeNPs.

X-ray diffraction (XRD)

XRD is a versatile analytical technique that is widely used for the structural analysis of materials, including magnetic nanoparticles (Ali et al., 2022). XRD was employed in this study to examine the structural attributes of the green-synthesized FeNPs. A broad peak centered around 2θ between 20 and 25° confirms the formation of amorphous iron nanoparticles, as shown in Figure 6.

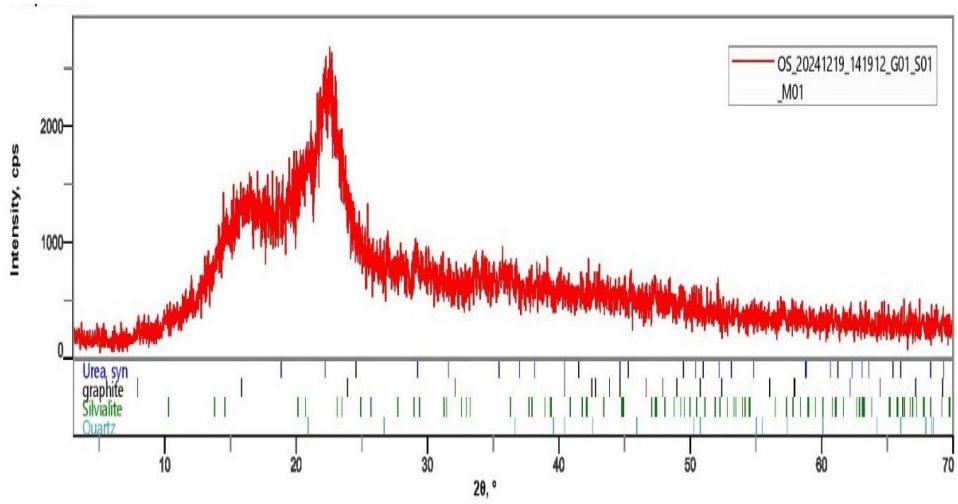

Figure 6. XRD of green-synthesized FeNPs from *F. capensis*.

Antioxidant activity

The antioxidant potential of the green-synthesized FeNPs was assessed using the DPPH free radical scavenging assay. This is a hydrogen atom transfer mechanism where the purple DPPH radical solution is reduced to produce stable yellow DPPH molecules. The absorption associated with this reduction process is measured at 517 nm, indicative of an antioxidant activity (Kingori et al., 2024). The FeNPs displayed substantial antioxidant activity, with a recorded IC_{50} value of 6.474 µg/mL (Figure 7). The antioxidant activity of nanoparticles relates to their capability to provide hydrogen atoms and unpaired electrons to the DPPH radical, thereby effectively neutralizing the target compound (Majeed et al., 2021).

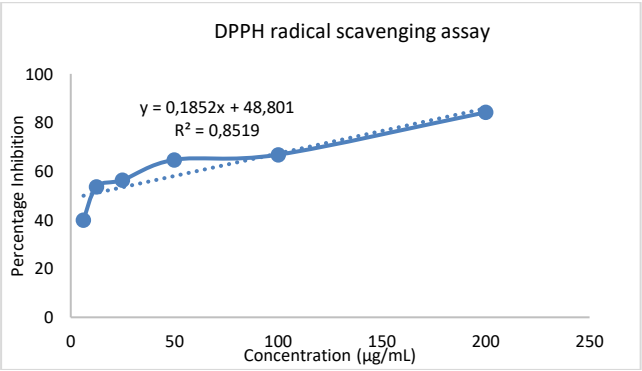

Figure 7. DPPH radical scavenging activity of the synthesized FeNPs. The data are presented as the means ± standard deviations (SD) (n = 3).

Antibacterial activity of FeNPs

The antibacterial efficacy of the green-synthesized iron nanoparticles (FeNPs) derived from *F. capensis* stem bark extract was assessed against Gram-positive (*Escherichia coli, Bacillus subtilis, Staphylococcus aureus*) and Gram-negative (*Pseudomonas aeruginosa, Klebsiella pneumoniae*) bacterial strains. *E. coli* is primarily linked to infections in the gastrointestinal and urinary tract, while *S. aureus* is associated with a range of skin and soft tissue infections (Frickmann et al., 2019). *P. aeruginosa* predominantly causes nosocomial infections such as pneumonia and infections of the urinary tract (UTIs) (Reynolds and Kollef, 2021). The FeNPs displayed measurable zones of inhibition against *E. coli* (22 ± 1.02 mm), *S. aureus* (18 ± 0.15 mm), and *K. pneumoniae* (15 ± 0.21 mm) at 250 µg/mL, while *P. aeruginosa* showed no inhibition at the tested concentrations (Table 2).

Minimum inhibitory concentration (MIC) findings corroborated these trends, with viable suppression of *E. coli* and *S. aureus* at 100 µg/mL, but no complete inhibition of *B. subtilis* or *K. pneumoniae* at this concentration (Table 3). This implies that the MICs of FeNPs against *B. subtilis* or *K. pneumoniae* are greater than 100 µg/mL. *P. aeruginosa* was excluded from the MIC table due to its complete resistance in the diffusion assay.

Table 2. Zone of inhibition (mm) of the green-synthesized FeNPs.

S/N	Bacteria strain	Zone of inhibition of microorganism (mm)			
		125 µg	250 µg	Co-amox. (30 µg)	Dist. H2O
	Bacillus Substilis	0±0.0	9 ± 0.40	29±2.51	0±0.0
	Escherichia coli	18 ± 0.12	22 ± 1.02	24±3.12	0±0.0
	Klebsiella pneumoniae	12± 0.41	15± 0.21	25±1.01	0±0.0
	Pseudomonas aeruginosa	0±0.0	0±0.0	22±2.03	0±0.0
	Staphylococcus aureus	12± 0.35	18 ± 0.15	27±1.56	0±0.0

Key: 0±0.0 = No activity (no zone of inhibition), Co-amox. = Amoxicillin clavulanate (Co-amoxiclav), Dist H_2O = Distilled water

Table 3. Minimum inhibitory concentration (MIC) of FeNPs against susceptible microorganisms.

S/N	Concentration (µg/mL)	*B. substilis*	*E. coli*	*K. pneumoniae*	*S. aureus*
	100.0	+	-	+	-
	75.0	+	+	+	+
	50.0	+	+	+	+
	25.0	+	+	+	+

"+" – Growth; "-" – no growth.

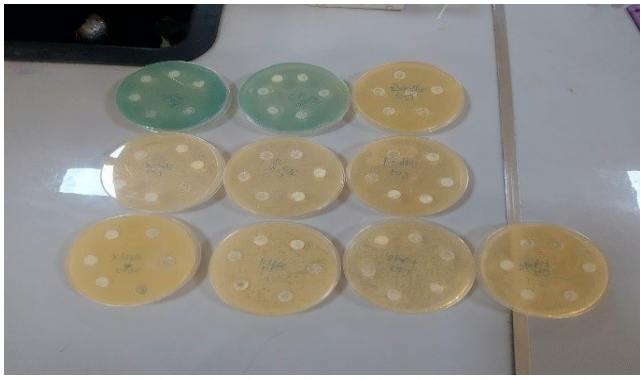

Figure 8. Agar plates for the antibacterial activity of green-synthesized FeNPs showing zones of inhibition.

Discussion

Studies on the green synthesis of iron nanoparticles (FeNPs) using plant extracts indicate that polyphenolic compounds, notably flavonoids and other phenolics, function both as reducing agents and as stabilizers. These phytochemicals facilitate the reduction of iron ions to elemental or oxide nanoparticles and inhibit particle aggregation (Saif et al., 2016; Sheta et al., 2024). Polyphenols are the predominant class employed in eco-friendly syntheses, mediating electron transfer to metal ions and providing surface capping that limits particle growth (Khoirotin et al., 2023; Zuhrotun et al., 2023). In the present work, FeNP formation is ascribed to reduction by bio-reductants in the *Ficus capensis* stem bark extract, which is known to be rich in polyphenolics and terpenoids (Mgbemena et al., 2022; Obodo and Tasie, 2022); the high concentration of these constituents in the reaction medium contributed to the substantial nanoparticle yield. Consistent with previous reports, increasing the concentration of plant extract—which raises the availability of reducing and capping phytochemicals—promotes more rapid nucleation and yields smaller nanoparticles (Abbai et al., 2016; Jiménez Pérez et al., 2017; Zuhrotun et al., 2023).

Formation of FeNPs was monitored by a time-dependent colour change of the reaction mixture. Immediately after the addition of *Ficus capensis* stem bark extract to ferric chloride, the solution darkened to brown and subsequently turned black (Figure 2), indicating phytochemical-mediated reduction of iron ions. The black appearance of the colloid is attributable to visible-region light absorption and the collective oscillation of free electrons of the nanoparticles' surface (surface plasmon resonance, SPR). This transition from dark brown to black is consistent with previous reports (Sahar et al., 2020; Elkhateeb et al., 2024; Ashrafi-Saiedlou et al., 2025). The synthesis of iron oxide nanoparticles is typically associated with a UV-visible wavelength range of 320–400 nm as reported by Ashrafi-Saiedlou et al. (2025). The study by Khan et al. (2025) showed an absorption maximum at 270 and 313 nm for FeNPs biosynthesized using *Citrus Limetta* agrowaste. Salim et al. (2025) reported a characteristic absorbance peak value of 292 nm for FeNPs synthesized using *Myristica fragrans* leaf extract. Slight variation in the absorption peaks may be attributed to different quantities of the reducing chemicals present in the extracts.

The FTIR peaks confirmed the capping of FeNPs by the phytochemicals present in the plant extract. The broad band at 3254 cm^{-1} is attributed to stretching vibrations of a phenolic or alcoholic hydroxyl group (O–H) of an organic acid or polyphenolic compound. This broad nature of the peak is due to the formation of inter- and intramolecular hydrogen bonds (Bhuiyan et al., 2020). Signals at 2922 cm^{-1} correspond to C–H stretching associated with CH_3 and CH_2 groups, 1603 cm^{-1} is consistent with the C=C (alkene) stretching vibration, while 1435 cm^{-1} represents methylene C-H bending bond and C=O stretching. The peak at 1297 cm^{-1} reflects a C–O- stretching, and that at 1018 cm^{-1} is assigned to C–O stretching. A similar pattern was observed in other studies (Khan et al., 2025; Salim et al., 2025), confirming the purity and homogeneity of our research.

The SEM analysis presented in Figure 6 demonstrated a variability in nanoparticle sizes, which can be attributed to the differing reducing abilities of the phytochemicals found in the extract. This finding aligns with the results reported by Bhutto et al. (2023), who observed subspherical and agglomerated iron nanoparticles with a rough and porous surface, synthesized using the leaf extract of *Ixora coccinea*. The XRD analysis indicated an absence of distinct diffraction peaks, which points to the amorphous nature of the produced nanoparticles (Figure 5) (Machado et al., 2015; Wei et al., 2017). The broad peak detected at 2θ values ranging from 20° to 25° implies the existence of organic capping agents derived from the plant extract, corroborating previous findings (Abdullah et al., 2023; Villagrán et al., 2024). Machado et al. (2015) also reported similar amorphous iron oxide nanoparticles.

Assessment of nanoparticle antioxidant capacity is critical for evaluating their potential to attenuate

oxidative stress and associated cellular damage, thereby contributing to the prevention of chronic disease, aging, and inflammatory conditions. Metal nanoparticles synthesized using secondary metabolites from plants have recently been proposed as alternatives to conventional therapeutics because of their biocompatibility, stability, and notable antioxidant activity (Kumar et al., 2020). The pronounced antioxidant activity observed for the FeNPs in this study is likely due to the nanoparticles' intrinsic ability to scavenge and reduce oxidized free radicals. Consequently, FeNPs synthesized from *Ficus capensis* stem bark extract represent promising antioxidant agents warranting further evaluation in targeted in vitro and in vivo models.

FeNPs possess excellent antimicrobial properties against a wide selection of microorganisms, including bacteria, fungi, and viruses (Zhang and Miao, 2024; Ashrafi-Saiedlou et al., 2025). *F. capensis*-biosynthesized FeNPs were effective at inhibiting the growth of some tested pathogenic bacteria, which include *Escherichia coli, Klebsiella pneumonia, Pseudomonas aeruginosa,* and *Staphylococcus aureus*. Similar results were obtained by Vitta et al. (2020), who stated that the biosynthesis of FeNPs using *Eucalyptus robusta* extract had a high potential for antibacterial activity against *Pseudomonas aeruginosa*, *Escherichia coli*, *Staphylococcus aureus*, and *Bacillus subtilis.* The bactericidal and bacteriostatic effects observed are consistent with previous research indicating that iron oxide nanoparticles possess intrinsic antibacterial properties that vary with organism type and nanoparticle physicochemical characteristics (Zhang and Miao, 2024). These disparities often stem from differences in bacterial cell envelope architecture, extra-chromosomally expressed morphological traits, etc., all of which can impede nanoparticle penetration into the bacterial cells (Dakal et al., 2016; Modi et al., 2023). Furthermore, the absence of activity against *P. aeruginosa* in this study may be a reflection of trends seen in other studies where intrinsic and extrinsic resistance mechanisms combine to reduce susceptibility to metal nanoparticles.

Mechanistic studies suggest that multiple pathways contribute to the antimicrobial efficacy of FeNPs. A primary mechanism reported in recent literature involves the generation of reactive oxygen species (ROS) that induce oxidative stress, damaging bacterial cell membranes, proteins, and nucleic acids (Dakal et al., 2016; Zhang and Miao, 2024). Our findings support this perspective, as zones of inhibition correlated with increasing nanoparticle concentration, suggesting enhanced oxidative interactions at higher doses. Previous work has also shown that nanoparticle physicochemical properties, such as surface charge and particle size, influence their antibacterial action (Dakal et al., 2016; Modi et al., 2023). Positively charged iron oxide nanoparticles have been reported to exhibit stronger antimicrobial effects through enhanced electrostatic attraction and cellular uptake compared with negatively charged counterparts (Zhang and Miao, 2024).

The differential inhibition patterns observed among tested bacteria and the complete resistance of *P. aeruginosa* may also be attributed to variations in oxidative stress responses and membrane repair mechanisms. *P. aeruginosa,* for instance, is known as a biofilm former with robust efflux systems that may contribute to its resilience against both conventional antibiotics and nanoparticle treatment (Thi et al., 2020; Hu and Chua, 2025). In contrast, the pronounced susceptibility of *E. coli* and *S. aureus* aligns with studies reporting strong inhibition of these organisms by iron oxide nanoparticles, likely due to more effective ROS penetration and membrane disruption (Gudkov et al., 2021). The antibacterial effectiveness of metal oxide nanoparticles is also influenced by factors such as concentration, size, distribution, and agglomeration. Higher concentrations of nanoparticle suspensions can enhance antibacterial activity due to increased specific surface area and tendency for penetration through cell barriers (Kadiyala et al., 2018).

Another important factor impacting antibacterial performance and concentration-dependent antimicrobial activity, as recorded in this study, is nanoparticle stability and aggregation state. Well-dispersed nanoparticles with a high specific surface area tend to exhibit improved contact with bacterial cells, increasing the production of reactive intermediates and enhancing antimicrobial action (Zhang and Miao, 2024). Recall that the MIC assay demonstrated the antibacterial efficacy of the FeNPs (Table 3). Complete inhibition (no visible growth) was observed at 100 µg/mL for *E. coli* and *S. aureus*, indicating strong bacteriostatic/bactericidal activities. *B. subtilis* and *K. pneumoniae* showed visible growth at 100 µg/mL. This implies that the MICs of the FeNPs against *B. subtilis* or *K. pneumoniae* is greater than 100 µg/mL, suggesting a deviation from the natural pattern where most Gram-positive isolates are generally more susceptible than their Gram-negative counterparts to the destructive effect of antimicrobial agents, suggesting an extrachromosomal mechanism of resistance (Esievo et al., 2018). Therefore, this study has demonstrated that FeNPs derived from *Ficus capensis* stem bark extract exhibited profound antibacterial activity against some clinically relevant microbial pathogens, although the degree of susceptibility varied across strains.

CONCLUSIONS

The synthesis of eco-friendly and sustainable nanoparticles by using green synthesis methods is promising, as cheap and easy starting materials are employed. The iron nanoparticles synthesized from *Ficus capensis* stem bark extract showed significant

antioxidant and antibacterial activities, reinforcing the plant's rich medicinal value, serving as a potential candidate in various drug research initiatives. Optimization of synthesis parameters and comprehensive toxicity assessments to enhance the therapeutic efficacy and safety of these nanoparticles for biomedical applications is necessary.

Acknowledgements: The authors acknowledge the contributions of staff in the Department of Pharmaceutical and Medicinal Chemistry, and the Department of Pharmaceutical Microbiology and Biotechnology, Afe Babalola University, Ado-Ekiti, for providing the facilities for conducting this research.

Authors Contributions: Uchenna Benjamin Okeke, Oscar Ifeanyichukwu Onyemaobi, and Ejiro Dowe designed and conducted the experiment. Uchenna Benjamin Okeke, Oscar, Ifeanyichukwu Onyemaobi, Ejiro Dowe, Bako Wunia'h, and Wande Michael Oluyemi analyzed the results. Uchenna Benjamin Okeke and Ejiro Dowe prepared, reviewed, and edited the manuscript. All authors have read and approved the final manuscript.

Conflict of Interest: The authors declare that there are no competing interests.

REFERENCES

Abbai, R., Mathiyalagan, R., Markus, J., Kim, Y.J., Wang, C., Singh, P., Ahn, S., Farh, M.E.A., and Yang, D.C. (2016). Green Synthesis of Multifunctional Silver and Gold Nanoparticles from the Oriental Herbal Adaptogen: Siberian Ginseng. *International Journal of Nanomedicine, 11*, 3131–3143. doi: 10.2147/IJN.S108549.

Abdullah, J.A.A., Díaz-García, Á., Law, J.Y., Romero, A., Franco, V., and Guerrero, A. (2023). Quantifying the structure and properties of nanomagnetic iron oxide particles for enhanced functionality through chemical synthesis. *Nanomaterials*, *13*, 2242. doi.org/10.3390/nano13152242

Achi, N.K., Chimaraoke, O., Ekeleme-Egedigwe, C.A., and Onyeanula, J.C. (2017). Phytochemical, Proximate Analysis, Vitamin and Mineral Composition of Aqueous Extract of Ficus capensis leaves in South Eastern Nigeria. *Journal of Applied Pharmaceutical Science,* 7(03), 117-122. doi: 10.7324/JAPS.2017.70319

Ali, A., Chiang, Y.W., and Santos, R.M. (2022). X-ray Diffraction Techniques for Mineral Characterization: A Review for Engineers of the Fundamentals, Applications, and Research Directions. *Minerals*, *12*, 205. https://doi.org/10.3390/min12020205

Ashrafi-Saiedlou, S., Rasouli-Sadaghiani, M., Fattahi, M., and Ghosta, Y. (2025). Biosynthesis and characterization of iron oxide nanoparticles fabricated using cell-free supernatant of *Pseudomonas fluorescens* for antibacterial, antifungal, antioxidant, and photocatalytic applications. *Scientific Reports*, *15,* 1018. https://doi.org/10.1038/s41598-024-84974-0

Bhuiyan, M.S.H., Miah, M.Y., Paul, S.C., Aka, T.D., Saha, O., Rahaman, M.M., Sharif, M.J. I., Habiba, O., and Ashaduzzaman, M. (2020). Green synthesis of iron oxide nanoparticle using *Carica papaya* leaf extract: Application for photocatalytic degradation of remazol yellow RR dye and antibacterial activity. *Heliyon*, *6*(8), e04603. https://doi.org/10.1016/j.heliyon.2020.e04603

Bhutto, A.A., Baig, J.A., Sirajuddin, Kazi, T.G., Sierra-Alvarez, R., Akhtar, K., and Samejo, S. (2023). Biosynthesis and analytical characterisation of iron oxide nanobiocomposite for in-depth adsorption strategy for the removal of toxic metals from drinking water. *Arabian Journal for Science and Engineering, 48*, 7411-7424. doi.org/10.1007/s13369-022-07477-y

Cho, E.J., Holback, H., Liu, K.C., Abouelmagd, S.A., Park, J., and Yeo, Y. (2013). Nanoparticle characterization: state of the art, challenges, and emerging technologies. *Molecular Pharmaceutics*, *10*(6), 2093–2110. https://doi.org/10.1021/mp300697h

Dakal, T.C., Kumar, A., Majumdar, R.S., and Yadav, V. (2016). Mechanistic Basis of Antimicrobial Actions of Silver Nanoparticles. *Frontiers in Microbiology*, 7, 1831.

Elkhateeb, O., Atta, M.B., and Mahmoud, E. (2024). Biosynthesis of iron oxide nanoparticles using plant extracts and evaluation of their antibacterial activity. *AMB Express*, *14*, 92. https://doi.org/10.1186/s13568-024-01746-9

Esievo, K.B., Anthony, S.O., Fatokun, O.T., and Kunle, O.F. (2018). *Ficus capensis* Thumb. (Moraceae): Review of Its Ethnomedicinal Uses, Pharmacological Activities and Phytochemical Constituents. *Archives of Current Research International*, *12*(3), 1–7. https://doi.org/10.9734/ACRI/2018/39495.

Frickmann, H., Hahn, A., Berlec, S., Ulrich, J., Jansson, M., Schwarz, N.G., Warnke, P., and Podbielski, A. (2019). On the Etiological Relevance of *Escherichia coli* and *Staphylococcus aureus* in Superficial and Deep Infections - A Hypothesis-Forming, Retrospective Assessment. *European Journal of Microbiology & Immunology*, *9*(4), 124–130. https://doi.org/10.1556/1886.2019.00021

Ghosh, S., Ahmad, R., Zeyaullah, M., Khare, S.K. (2021). Microbial nano-factories: Synthesis and biomedical applications. *Frontiers in Chemistry, 9*, 194. https://doi.org/10.3389/fchem.2021.626834

Gudkov, S.V., Burmistrov, D.E., Serov, D.A., Rebezov, M.B., Semenova, A.A., and Lisitsyn, A.B. (2021). Do Iron Oxide Nanoparticles Have Significant Antibacterial Properties? *Antibiotics (Basel, Switzerland), 10*(7), 884. https://doi.org/10.3390/antibiotics10070884

Hossain, T.J. (2024). Methods for screening and evaluation of antimicrobial activity: A review of protocols, advantages, and limitations. *European Journal of Microbiology & Immunology, 14*(2), 97–115. https://doi.org/10.1556/1886.2024.00035

Hu, M., and Chua, S.L. (2025). Antibiotic-Resistant *Pseudomonas aeruginosa*: Current Challenges and Emerging Alternative Therapies. *Microorganisms*, *13*(4), 913. https://doi.org/10.3390/microorganisms13040913

Jiménez Pérez, Z.E., Mathiyalagan, R., Markus, J., Kim, Y.J., Kang, H.M., Abbai, R., Seo, K.H., Wang, D., Soshnikova, V., and Yang, D.C. (2017). Ginseng-Berry-Mediated Gold and Silver Nanoparticle Synthesis and Evaluation of Their in Vitro Antioxidant, Antimicrobial, and Cytotoxicity Effects on Human Dermal Fibroblast and Murine Melanoma Skin Cell Lines. *International Journal of Nanomedicine, 12*, 709–723. doi: 10.2147/IJN.S118373.

Kadiyala, U., Kotov, N.A., and VanEpps, J.S. (2018). Antibacterial Metal Oxide Nanoparticles: Challenges in Interpreting the Literature. *Current Pharmaceutical Design, 24*(8), 896-903. https://doi.org/10.2174/1381612824666180219130659

Karunakaran, G., Sudha, K.G., Ali, S., Cho, E.B. (2023). Biosynthesis of Nanoparticles from Various Biological Sources and Its Biomedical Applications. *Molecules*, *28*(11), 4527. doi: 10.3390/molecules28114527.

Khan, M.A., Ahmed, M., Abu-Hussien, S.H., Zahid, M.U., and Alharbi, B.F. (2025). Green synthesis of iron oxide nanoparticles (Fe_2O_3-NPs) from *Citrus Limetta* agrowaste for biological and photocatalytic applications. *Scientific Reports*, *15*(1), 33107. https://doi.org/10.1038/s41598-025-17750-3

Khoirotin, Faaizatunnisa, N., and Munasir. (2023). Green synthesis of Fe_3O_4 nanoparticles using green betel leaf extract for methylene blue adsorption. *Natural and Life Sciences Communications, 22*(3), e2023042**.**

Kingori, S., Cheruiyot, S., Kirui, A., Uwamahoro, R., and Mwangi, A. (2024). Optimization and Validation of a Simple Spectrophotometric Based DPPH Method for Analysis of Antioxidant Activity in Aerated, Semi-Aerated and Non-Aerated Tea Products. *Open Journal of Applied Sciences*, *14*, 2207-2222. doi: 10.4236/ojapps.2024.148148.

Kumar, H., Bhardwaj, K., Nepovimova, E., Kuča, K., Dhanjal, D. S., Bhardwaj, S., Bhatia, S. K., Verma, R., and Kumar, D. (2020). Antioxidant Functionalized Nanoparticles: A Combat against Oxidative Stress. *Nanomaterials (Basel, Switzerland), 10*(7), 1334. https://doi.org/10.3390/nano10071334

Machado, S., Pacheco, J.G., Nouws, H.P., Albergaria, J.T., and Delerue-Matos, C. (2015). Characterization of green zero-valent iron nanoparticles produced with tree leaf extracts. *The Science of the Total Environment, 533*, 76–81. https://doi.org/10.1016/j.scitotenv.2015.06.091

Majeed, S., Mohammed D., Mohammad, N.M.I., Siti, H.S., Ansari, M.T., Nanda, A., and Ahmad, G. (2021). Bacteria Mediated Synthesis of Iron Oxide Nanoparticles and Their Antibacterial, Antioxidant, Cytocompatibility Properties. *Journal of Cluster Science, 32*, 1083–1094. https://doi.org/10.1007/s10876-020-01876-7

Mgbemena, N.M., Akoh, O.U., Obodo, G.A., and Nwakwue, K. (2022). Determination of the Phytochemicals, Minerals, Proximate and Antibacterial Constituents of the Leaf, Stem, Root and Seed of *Ficus capensis* (bush fig). *Journal of Chemical Society of Nigeria, 47*(1), 179 – 189.

Mishra, A., Pradhan, D., Halder, J., Biswasroy, P., Rai, V.K., Dubey, D., Kar, B., Ghosh, G., and Rath, G. (2022). Metal nanoparticles against multi-drug-resistance bacteria. *Journal of Inorganic Biochemistry, 237*, 111938. https://doi.org/10.1016/j.jinorgbio.2022.111938

Modi, S.K., Gaur, S., Sengupta, M., and Singh, M.S. (2023). Mechanistic insights into nanoparticle surface-bacterial membrane interactions in overcoming antibiotic resistance. *Frontiers in Microbiology, 14*, 1135579. doi: 10.3389/fmicb.2023.1135579

NMPP. (2026). *Ficus capensis.* www.nmppdb.com.ng/species-details?specy=%20ficus-capensis.

Obodo, N.C., and Tasie, F.O. (2022). Evaluation of the phytochemical contents of stem-bark and leaf extract of *Ficus capensis. IAA Journal of Scientific Research*, *8*(1), 83-89.

Okafor, V.N., Kehinde, D.O., Akinyele, A.B., and Modozie, B.U. (2024). Synthesis of Nanochitosan from Cambarus Bartonii Waste and its Utilization in The Removal of Polycyclic Aromatic Hydrocarbons in Surface Water from Ifite Ogwari, Southeastern Nigeria. *Nanochemistry Research, 9*(1), 42-54. doi: 10.22036/NCR.2024.01.06

Okeke, U.B., Igbinaduwa, P., Aladesanmi, J.A., Mzozoyana, V., and Kehinde, I.O. (2026). GCMS-based phytochemical profiling, antioxidant and anti-inflammatory activity of triterpenoid-rich hydroethanolic extract and fractions of *Ficus Sur* (Forrsk) stem bark. *Natural and Life Sciences Communications*, *25*(1), e2026012.

Omodamiro, O.D., Ajah, O., Jimoh, M.A., and Ewa-Ibe, C. (2021). Evaluation of sub-chronic toxicity, anti-inflammatory and diuretic effect of ethanol leaves extract *Ficus capensis* in albino rat. *Animal Research International, 18*(2), 4073–4082.

Osman, A.I., Zhang, Y., Farghali, M., Rashwan, A.K., Eltaweil, A.S., Abd El-Monaem, E.M., Mohamed, I.M.A, Badr, M.M., Ihara, I., Rooney, D.W., and Yap. P.S. (2024). Synthesis of green nanoparticles for energy, biomedical, environmental, agricultural, and food applications: A review. *Environmental Chemistry Letters, 22*, 841–887. https://doi.org/10.1007/s10311-023-01682-3.

Reynolds, D., and Kollef, M. (2021). The Epidemiology and Pathogenesis and Treatment of Pseudomonas aeruginosa Infections: An Update. *Drugs, 81*(18), 2117–2131. https://doi.org/10.1007/s40265-021-01635-6

Sahar, T., Munir, H. Zia, Z., Nageen, Rafiq, N., Shafiq, N., Aleem, S., and Aslam S. 2020. Ecofriendly Green Synthesis of Iron Oxide Nanoparticles Using *citrus sinensis*. *Frontiers in Chemical Sciences*, *1*(1), 21-28.

Sahoo, S.K., Agarwal, K., Singh, A.K., Polke, B.G., and Raha, K.C. (2010). Characterization of γ- and α-Fe_2O_3 nano powders synthesized by emulsion precipitation-calcination route and rheological behaviour of α-Fe_2O_3. *International Journal of Engineering, Science and Technology*, *2*(8), 118-126. doi: 10.4314/ijest.v2i8.63841

Saif, S., Tahir, A., and Chen, Y. (2016). Green Synthesis of Iron Nanoparticles and Their Environmental Applications and Implications. *Nanomaterials (Basel, Switzerland), 6*(11), 209. https://doi.org/10.3390/nano6110209

Salehirozveh, M., Dehghani, P., and Mijakovic, I. (2024). Synthesis, Functionalization, and Biomedical Applications of Iron Oxide Nanoparticles (IONPs). *Journal of Functional Biomaterials, 15*(11), 340. https://doi.org/10.3390/jfb15110340

Salim, S., Hari, N., Sudhi, S., and Nair, A.J. (2025). Green synthesis, characterisation and bioactivity of iron oxide nanoparticles using *Myristica fragrans* leaf extract. *The Microbe, 8*, 100481. https://doi.org/10.1016/j.microb.2025.100481

Sánchez-Moreno, C., Larrauri, J.A., and Saura-Calixto, F. (1998). A procedure to measure the antiradical efficiency of polyphenols. *Journal of the Science of Food and Agriculture*, *79,* 270–276.

Sheta, M.H., Abd El-Wahed, A.H., Elshaer, M.A., Bayomy, H.M., Ozaybi, N.A., Abd-Elraheem, M.A., El-Sheshtawy, A.N.A., El-Serafy, R.S., and Moustafa, M.M. (2024). Green Synthesis of Zinc and Iron Nanoparticles Using *Psidium guajava* Leaf Extract Stimulates Cowpea Growth, Yield, and Tolerance to Saline Water Irrigation. *Horticulturae, 10*(9), 915. https://doi.org/10.3390/horticulturae10090915

Sofowora, A. (1993). Screening Plants for Bioactive Agents. p.134-156. In: Medicinal Plants and Traditional Medicine in Africa. Spectrum Books, Ibadan.

Tehri, N., Vashishth, A., Gahlaut, A., and Hooda, V. (2022). Biosynthesis, antimicrobial spectra and applications of silver nanoparticles: Current progress and future prospects. *Inorganic and Nano-Metal Chemistry, 52*, 1–19. https://doi.org/10.1080/24701556.2020.1862212

Thi, M.T.T., Wibowo, D., and Rehm, B.H. A. (2020). Pseudomonas aeruginosa Biofilms. *International Journal of Molecular Sciences, 21*(22), 8671. https://doi.org/10.3390/ijms21228671

Trease, G.E., and Evans, W.C. (2003). Pharmacognosy. Saunders, London.

Villagrán, Z., Anaya-Esparza, L.M., Velázquez-Carriles, C.A., Silva-Jara, J.M., Ruvalcaba-Gómez, J.M., Aurora-Vigo, E.F., Rodríguez-Lafitte, E., Rodríguez-Barajas, N., Balderas-León,

I., and Martínez-Esquivias, F. (2024). Plant-Based Extracts as Reducing, Capping, and Stabilizing Agents for the Green Synthesis of Inorganic Nanoparticles. *Resources*, *13*(6), 70. https://doi.org/10.3390/resources13060070

Vitta, Y., Figueroa, M., Calderon, M., and Ciangherotti, C. (2020). Synthesis of iron nanoparticles from aqueous extract of *Eucalyptus robusta* Sm and evaluation of antioxidant and antimicrobial activity. *Materials Science for Energy Technologies*, *3*, 97-103. doi:10.1016/j.mset.2019.10.014

Wahab, S., Salman, A., Khan, Z., Khan, S., Krishnaraj, C., and Yun, S.I. (2023). Metallic Nanoparticles: A Promising Arsenal against Antimicrobial Resistance-Unraveling Mechanisms and Enhancing Medication Efficacy. *International Journal of Molecular Sciences, 24*(19), 14897. doi: 10.3390/ijms241914897.

Wei, Y., Fang, Z., Zheng, L., and Tsang, E.P. (2017). Biosynthesized iron nanoparticles in aqueous extracts of *Eichhornia crassipes* and its mechanism in the hexavalent chromium removal. *Applied Surface Science*, *399*, 322-329. Doi.org/10.1016/j.apsusc.2016.12.090

Wiegand, I., Hilpert, K., and Hancock, R.E. (2008). Agar and broth dilution methods to determine the minimal inhibitory concentration (MIC) of antimicrobial substances. *Nature Protocols, 3*(2), 163–175. https://doi.org/10.1038/nprot.2007.521

Zhang, T.G., and Miao, C.Y. (2024). Iron Oxide Nanoparticles as Promising Antibacterial Agents of New Generation. *Nanomaterials (Basel, Switzerland). 14*(15), 1311. https://doi.org/10.3390/nano14151311

Zuhrotun, A., Oktaviani, D.J., and Hasanah, A.N. (2023). Biosynthesis of Gold and Silver Nanoparticles Using Phytochemical Compounds. *Molecules*, *28*(7), 3240. https://doi.org/10.3390/molecules28073240

THIS PAGE INTENTIONALLY LEFT BLANK